Brigitte I. Frohnert,[1] Eric K. Long,[2] Wendy S. Hahn,[2] and David A. Bernlohr[2]

Glutathionylated Lipid Aldehydes Are Products of Adipocyte Oxidative Stress and Activators of Macrophage Inflammation

Obesity-induced insulin resistance has been linked to adipose tissue lipid aldehyde production and protein carbonylation. *Trans*-4-hydroxy-2-nonenal (4-HNE) is the most abundant lipid aldehyde in murine adipose tissue and is metabolized by glutathione *S*-transferase A4 (GSTA4), producing glutathionyl-HNE (GS-HNE) and its metabolite glutathionyl-1,4-dihydroxynonene (GS-DHN). The objective of this study was to evaluate adipocyte production of GS-HNE and GS-DHN and their effect on macrophage inflammation. Compared with lean controls, GS-HNE and GS-DHN were more abundant in visceral adipose tissue of *ob/ob* mice and diet-induced obese, insulin-resistant mice. High glucose and oxidative stress induced production of GS-HNE and GS-DHN by 3T3-L1 adipocytes in a GSTA4-dependent manner, and both glutathionylated metabolites induced secretion of tumor necrosis factor-α from RAW 264.7 and primary peritoneal macrophages. Targeted microarray analysis revealed GS-HNE and GS-DHN induced expression of inflammatory genes, including C3, C4b, c-Fos, igtb2, Nfkb1, and Nos2. Transgenic overexpression of GSTA4 in mouse adipose tissue led to increased production of GS-HNE associated with higher fasting glucose levels and moderately impaired glucose tolerance. These results indicated adipocyte oxidative stress results in GSTA4-dependent production of proinflammatory glutathione metabolites, GS-HNE and GS-DHN, which may represent a novel mechanism by which adipocyte dysfunction results in tissue inflammation and insulin resistance.

Diabetes 2014;63:89–100 | DOI: 10.2337/db13-0777

The effect of obesity on development of insulin resistance and cardiovascular risk has been associated with increased oxidative stress and a state of chronic low-grade inflammation in adipose tissue (1). Although pathologic states of oxidative stress and inflammation are clearly related in diseases spanning various biological tissues and systems, evidence for directionality and mechanism of interplay has remained elusive.

Overnutrition causes increased endothelial reticulum stress and adipose tissue mitochondrial dysfunction (2). This leads to decreased efficiency of oxygen consumption

[1]Department of Pediatrics, University of Minnesota, Minneapolis, MN
[2]Department of Biochemistry, Molecular Biology and Biophysics, University of Minnesota, Minneapolis, MN

Corresponding author: David A. Bernlohr, bernl001@umn.edu.

Received 15 May 2013 and accepted 15 September 2013.

This article contains Supplementary Data online at http://diabetes.diabetesjournals.org/lookup/suppl/doi:10.2337/db13-0777/-/DC1.

B.I.F. and E.K.L. contributed equally to this work.

and electron transport, culminating in increased production of superoxide anion (3,4). Superoxide dismutase converts superoxide anion to hydrogen peroxide (H_2O_2) that can be further metabolized by catalase or glutathione peroxidases, forming oxygen and water (5–8). Alternatively, H_2O_2 is subject to nonenzymatic degradation via iron-mediated Fenton chemistry producing hydroxyl radical (9), the reactive oxygen intermediate responsible for lipid peroxidation of polyunsaturated fatty acids (10).

Oxidative stress–induced lipid peroxidation results in production of reactive α,β-unsaturated aldehydes (10). These react with cysteine, lysine, and histidine residues of proteins via Michael addition and Schiff base formation in a process termed protein carbonylation (11). Protein function and abundance is influenced by protein carbonylation (12,13), suggesting a mechanism by which oxidative stress may cause mitochondrial dysfunction or other changes in cell metabolism and signaling. Specifically, *trans*-4-hydroxy-2-nonenal (4-HNE) inhibits coupled respiration in isolated mitochondria and carbonylates mitochondrial proteins (2).

Protection against carbonylation-induced mitochondrial dysfunction is accomplished by a number of phase I and phase II enzymes that metabolize lipid aldehydes through oxidation, reduction, or glutathionylation. Glutathionylation via glutathione-*S*-transferase A4 (GSTA4) may play a particularly important role in the metabolism of lipid aldehydes in adipose tissue because obesity-induced alterations in adipose tissue oxidative stress and inflammatory status correlate strongly with down-regulation of GSTA4 (14). Specifically, 4-HNE and other lipid aldehydes, such as *trans*-4-oxo-2-nonenal (4-ONE), are glutathionylated by GSTA4, exported rapidly in an ATP-dependent manner by RLIP76, and excreted in urine (15,16). Alternatively, GS-HNE (and GS-ONE) can be further reduced by aldoketoreductase to glutathionyl-1, 4-dihydroxynonene (GS-DHN), which is also exported by RLIP76 (17).

Although glutathione metabolism provides a protective clearance mechanism, recent studies suggest glutathionylated lipids have proinflammatory signaling properties. In studies examining the role of aldose reductase in inflammation, cells treated with a cell-permeable ethyl ester of GS-DHN induced nuclear factor-κB (NF-κB) signaling in RAW 264.7 macrophages (18). Further, injection of nonesterified GS-HNE into murine peritoneal cavities resulted in leukocyte infiltration and proinflammatory leukotriene production (19). Because nonesterified GS-HNE is poorly membrane soluble (20), there may be a receptor-mediated mechanism for its inflammatory properties.

To characterize glutathione metabolism in obesity-induced inflammation, GS-HNE and GS-DHN were quantified by liquid chromatography–tandem mass spectrometry (LC-MS/MS), and the inflammatory potential of each was measured using cell culture systems. In addition, a transgenic mouse model was produced whereby GSTA4 was overexpressed in adipose tissue and GS-HNE/GS-DHN evaluated. The results support the hypothesis that glutathione metabolites of lipid aldehydes provide a novel mechanistic link between adipocyte oxidative stress and local adipose tissue inflammation.

RESEARCH DESIGN AND METHODS

Materials

Nonesterified GS-HNE, GS-HNE-d3, and leukotriene C4 (LTC_4)-d_5 were purchased from Cayman Chemical (Ann Arbor, MI). Glutathione, butylated hydroxytoluene, and sodium borohydride ($NaBH_4$) were purchased from Sigma-Aldrich (St. Louis, MO).

Synthesis of GS-DHN

GS-HNE was incubated with 50 mmol/L $NaBH_4$ in ethanol for 1 h at 23°C to reduce the aldehyde, dried under nitrogen, and resuspended in 0.1% acetic acid, eliminating excess $NaBH_4$. Product was applied to a Strata-X solid-phase extraction cartridge, washed with water, and then eluted with methanol. Methanolic extract was dried under nitrogen and resuspended in water. GS-DHN was quantified spectrophotometrically using the GS-HNE calibration curve. Recovery was 33–67%, and product was >99% pure as determined by direct infusion MS.

Cell Culture

3T3-L1 preadipocytes were cultured and differentiated into adipocytes as described previously (21,22) and used on day 8 after differentiation. For low-glucose experiments, cells were grown in low-glucose (5.5 mmol/L) Dulbecco's modified Eagle's medium (DMEM) or standard, high-glucose (25 mmol/L) DMEM from time of plating, with media changed daily. GSTA4-silenced (knockdown [KD]) and GSTA4 overexpressing (OE) 3T3-L1 adipocytes and their respective control cell lines were generated as described previously (12) and were grown and differentiated (21), with the addition of blasticidin (1 μg/mL) for GSTA4 KD and scrambled cells and geneticin (400 μg/mL) for OE and pcDNA cells from time of plating until time of cell confluence and addition of 1 μg/mL troglitazone to the differentiation cocktail. RAW 264.7 macrophages (American Type Culture Collection) were grown in DMEM containing 10% FBS.

Generation of GSTA4 Transgenic Mice

Male C57Bl/6J wild-type and *ob*/*ob* mice were purchased from The Jackson Laboratory (Bar Harbor, ME). GSTA4 transgenic mice were generated from C57Bl/6J mice at the University of Minnesota Mouse Genetics Laboratory (Minneapolis, MN). The HA-tagged GSTA4 transgene is under the FABP4 promoter (provided by Dr. Ormond MacDougald, Ann Arbor, MI). Mice were weaned at 3 weeks of age onto a high-fat diet (Bioserve Industries, Frenchtown, NJ; No. F3282: 20% protein, 35.5% fat, 36.3% carbohydrate by weight, 60% fat by calories) or

standard chow (Teklad Global, Madison WI; 2018: 18.6% protein, 6% fat, 44% carbohydrate by weight), maintained at 70°F on a 14:10-h light-dark cycle, and fed ad libitum. At 15–20 weeks of age, animals were fasted for 4 h and underwent glucose tolerance testing (0.5 g glucose/kg) and insulin tolerance testing (1.0 unit/kg). Blood glucose was measured using the OneTouch Ultra glucometer (LifeScan, Inc.). Mice were killed 1 week later by CO_2 asphyxiation. Epididymal fat pads were harvested, flash frozen in liquid nitrogen, and stored at −80°C. All procedures were reviewed and approved by University of Minnesota Institutional Animal Care and Use Committee.

Isolation and Culture of Peritoneal Macrophages

C57Bl/6J mice were injected intraperitoneally with 3% thioglycollate (2 mL). After 4 days, peritoneal cells were collected by lavage and seeded in RPMI medium with 10% FBS. After 6 h, nonadherent cells were removed by rinsing with PBS. Adherent macrophages were grown in RPMI with 10% FBS and 1 μg/mL lipopolysaccharide (LPS) for 18 h, and then treated for 24 h with 10 μmol/L GS-HNE or 10 μmol/L GS-DHN in RPMI plus 10% FBS.

Adipose Tissue Glutathione Metabolite Content

Adipose tissue (~100 mg) was homogenized and incubated with 1.5 pmol GS-HNE-d_3 as the internal standard. Samples were vortexed, centrifuged at 3,800 rpm for 10 min at 4°C, and loaded on Strata-X solid-phase extraction cartridges preconditioned with methanol and equilibrated with water. Columns were washed with water. Glutathione metabolites were eluted with 100% methanol, dried under nitrogen, and resuspended in 25 μL methanol for LC-MS/MS analysis. GS-HNE was quantified by LC-MS/MS, similar to Long et al. (23).

Cellular Glutathione Metabolite Production

3T3-L1 adipocytes or RAW 264.7 macrophages were treated with 500 μmol/L H_2O_2 in Krebs-Ringer HEPES buffer (KRHB) containing 1% FBS for 1 h. Cell culture media was removed, spiked with 1 pmol GS-HNE-d_3 and prepared identically to tissue samples.

Glutathione Metabolite–Induced Leukotriene C_4 Production

Primary peritoneal macrophages were pretreated 18 h with 1 μg/mL LPS and were washed and treated with 10 μmol/L GS-HNE or GS-DHN in KRHB/0.1% FBS for 2 h. Cell culture media was removed and spiked with 1 pmol LTC_4-d_5 and then prepared, as described above, for LC-MS/MS analysis.

Glutathione Metabolite-Induced Tumor Necrosis Factor-α Production

RAW 264.7 or primary peritoneal macrophages were pretreated 24 h with 1 μg/mL LPS, followed by PBS wash. Macrophages were treated with GS-HNE or GS-DHN for 24 h in DMEM/0.1% FBS. Media was removed and frozen. Five microliters of media were assayed for tumor necrosis factor-α (TNF-α) content by ELISA kit from BD Biosciences (San Diego, CA).

RNA Preparations and RT-PCR

Total RNA was isolated from peritoneal macrophages by lysis in TRIzol (Invitrogen, Carlsbad, CA), according to the manufacturer's directions. RNA was further purified using the RNeasy Mini Kit (Qiagen, Valencia, CA). cDNA was generated from ~0.5 μg RNA using RT^2 First Strand kit (Qiagen), followed by real-time PCR with 96-well RT^2 profiler Mouse Inflammatory Response & Autoimmunity PCR array (Qiagen).

Real-Time RT-PCR

RNA was isolated from ~0.2 g mouse epididymal adipose tissue using Trizol (Invitrogen), according to the manufacturer's instructions. After DNase treatment, cDNA was synthesized using the iScript cDNA synthesis kit (BioRad). Relative quantification of mRNAs was performed by real-time PCR using iQ SYBR green Supermix and MyiQ detection system (BioRad). Primers for target genes were mGSTA4: forward: 5′-CGCTTTCAGGAGAGGGAAGTTG-3′ and reverse: 5′-AGGAACAAACCAGGAAACGTTAC-3′.

Enzymatic Assay of GSTA4

Epididymal fat pads from GSTA4 transgenic or wild-type mice were homogenized and protein concentration determined by bicinchoninic acid assay Sigma-Aldrich. Homogenates were diluted to 0.1 mg/mL and incubated with 1 mmol/L glutathione and 1 μmol/L 4-HNE for 1 min. Reaction was stopped by acetic acid (1% final concentration) and incubated with GS-HNE-d_3. Homogenates were subjected to solid-phase extraction and quantified by LC-MS/MS, as described above. Total GST activity was determined by the amount of GS-HNE produced per milligram of protein per minute (nmol/mg/min).

Statistical Analysis

All analyses were performed using Prism 6.0 software (GraphPad Software, La Jolla CA). Data were graphed as means ± SEM. Comparisons among groups were made using the Student *t* test with equal variance.

RESULTS

GS-HNE/GS-DHN in Murine Adipose Tissue

Adipose tissue was assayed for GS-HNE/GS-DHN in chow-fed, high fat–fed, and *ob/ob* mice. GS-HNE was significantly increased in high fat–fed (6.9-fold) and *ob/ob* mice (6.2-fold) compared with chow-fed mice (Fig. 1*A*). GS-DHN was significantly increased in *ob/ob* mice (4.3-fold) and showed a trend toward increased levels in high fat–fed mice (14.8-fold) (Fig. 1*B*).

GS-HNE/GS-DHN Production in 3T3-L1 Cell Lines

To characterize cell-specific formation of GS-HNE and GS-DHN, 3T3-L1 adipocytes or RAW 264.7 macrophages were treated with H_2O_2 to induce oxidative stress.

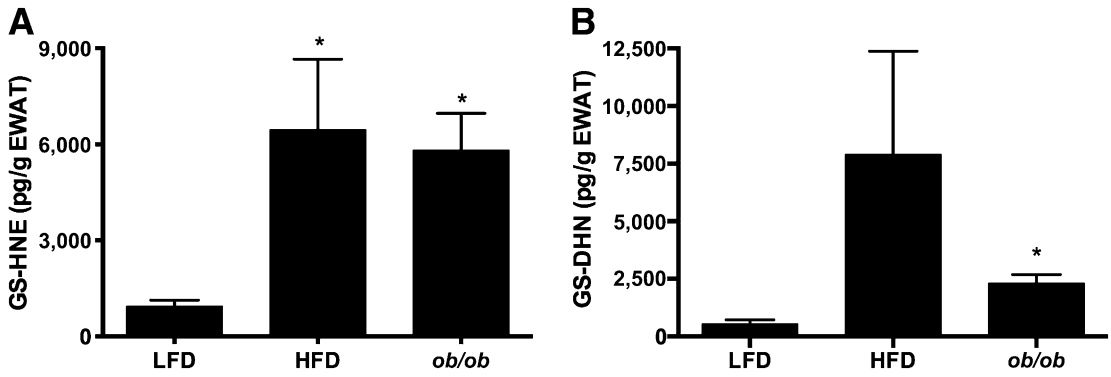

Figure 1—GS-HNE and GS-DHN content of mouse adipose tissue. Epididymal white adipose tissue (EWAT) was harvested from wild-type C57Bl/6J mice fed a low-fat diet (LFD) or a high-fat diet (HFD) and from *ob/ob* mice fed a low-fat diet (*ob/ob*) and assayed for GS-HNE (*A*) and GS-DHN (*B*) using LC-MS/MS. **P* < 0.05. HFD, high-fat diet; LFD, low-fat diet.

When 3T3-L1 adipocytes were used, GS-HNE (Fig. 2*A*) and GS-DHN (Fig. 2*B*) levels were increased (12-fold and 6-fold, respectively) in response to H_2O_2 treatment. In contrast, GS-HNE was not detected in control or treated RAW 264.7 macrophages, and GS-DHN levels did not increase in response to H_2O_2 (Fig. 2*A*). Furthermore, GS-HNE was not detected in primary peritoneal macrophages basally or in response to inflammatory stimuli (results not shown). These results suggested that adipocytes are the primary GS-HNE/GS-DHN–producing cells in adipose tissue.

Elevated serum glucose levels are associated with increased production of reactive oxygen species in a variety of tissues (24). In model systems, growth in high-glucose medium is associated with increased oxidative stress and insulin resistance (25). To test the effect of hyperglycemic conditions on lipid peroxidation in cultured adipocytes, 3T3-L1s were cultured in low- or high-glucose media from initial plating through differentiation. Adipocytes cultured in high-glucose media displayed larger and more abundant lipid droplets relative to those grown in low-glucose media, consistent with previous observations (Fig. 3*A*) (25). Adipocytes maintained in low- or high-glucose media were further challenged with H_2O_2 for 2 h on day 8 of differentiation. H_2O_2 treatment induced increased production of GS-HNE in low-glucose (9-fold, from 50 ± 8 to 460 ± 140 pg/mL; $P < 0.05$) and high-glucose (16-fold, from 65 ± 9 to 1,100 ± 200 pg/mL; $P < 0.001$) conditions (Fig. 3*B*). Production of GS-DHN increased with H_2O_2 treatment in low-glucose (4-fold, 150 ± 30 to 670 ± 270 pg/mL; but this was not significant, $P = 0.11$) and was significantly increased in high-glucose conditions (11-fold, 220 ± 90 to 2,500 ± 600 pg/mL; $P < 0.05$) (Fig. 3*C*). In untreated cells, high-glucose media generated slightly higher GS-HNE and GS-DHN relative to low-glucose media (65 ± 9 vs. 50 ± 8 pg/mL and 220 ± 90 vs. 150 ± 30 pg/mL, respectively); however, this was not significant. In combination with H_2O_2 treatment, however, high-glucose media resulted in increased GS-HNE production by 2.3-fold (1,100 ± 200 vs. 460 ± 140 pg/mL; $P < 0.05$) and GS-DHN was increased 3.7-fold (2,500 ± 600 vs. 670 ± 270 pg/mL;

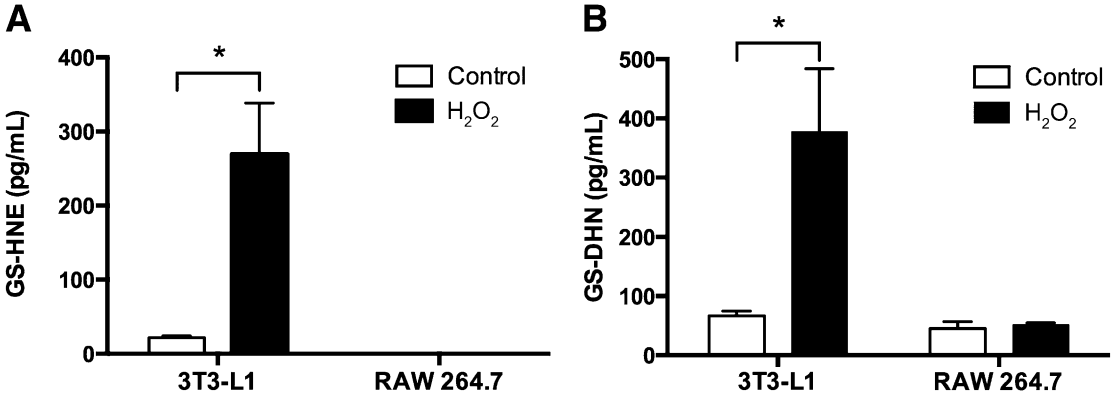

Figure 2—Production of GS-HNE (*A*) and GS-DHN (*B*) by 3T3-L1 adipocytes and RAW 264.7 macrophages. The indicated cells were treated with 500 μmol/L H_2O_2 for 4 h, and glutathionylated metabolite secretion into the medium was quantified by LC-MS/MS. **P* < 0.05.

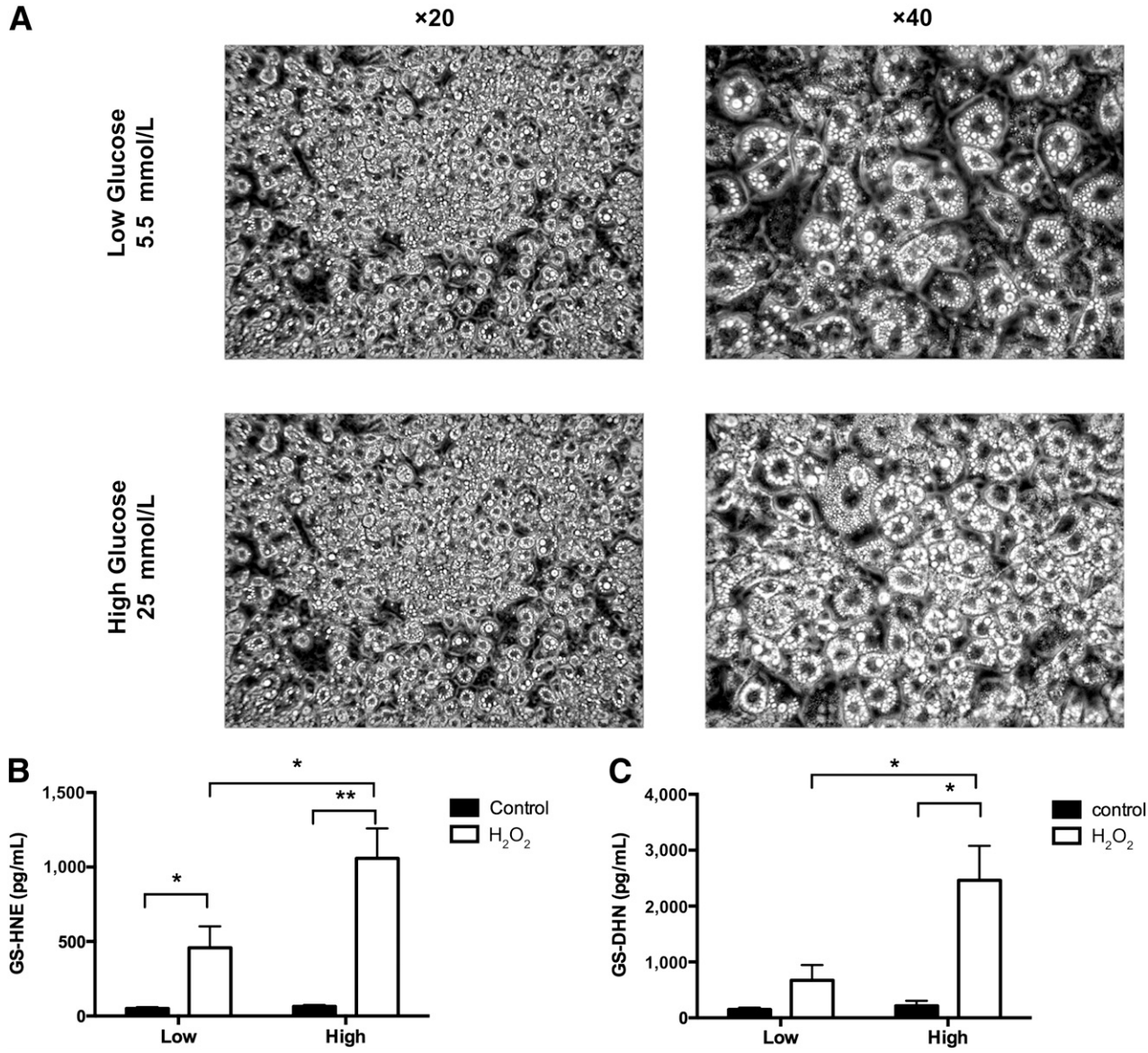

Figure 3—Production of GS-HNE and GS-DHN by 3T3-L1 adipocytes grown in low or high glucose in response to H_2O_2 treatment. *A*: Lipid droplet number and size were increased in adipocytes grown in high-glucose conditions, shown at original magnification ×20 and ×40. 3T3-L1 adipocytes were grown in low (5.5 mmol/L) or high (25 mmol/L) glucose conditions, treated with 500 μmol/L H_2O_2 for 2 h, and GS-HNE (*B*) and GS-DHN (*C*) were assayed in the supernatant by LC-MS/MS (n = 5–7). *P < 0.05, **P < 0.01.

$P < 0.05$) relative to low-glucose media. These results demonstrate a synergistic effect of H_2O_2 treatment under high-glucose conditions (Fig. 3*B* and *C*).

The enzyme primarily responsible for glutathionylation of 4-HNE, GSTA4, is implicated as an important factor in obesity-induced insulin resistance and metabolic dysfunction (2). To evaluate GSTA4-mediated production of GS-HNE/GS-DHN, GSTA4 KD and GSTA4 OE cell lines were challenged with H_2O_2. H_2O_2 treatment resulted in increased production of GS-HNE (6-fold, from 390 ± 50 to 2,400 ± 80 pg/mL; $P < 0.0001$) and GS-DHN (15-fold, from 530 ± 80 to 8,000 ± 1,400 pg/mL; $P < 0.01$) in GSTA4 KD (Fig. 4*A* and *B*). However, this increase was significantly less than the increased production of GS-HNE (20-fold, from 560 ± 20 to 11,000 ± 400 pg/mL; $P < 0.0001$) and GS-DHN (27-fold, from 510 ± 60 to 14,000 ± 400 pg/mL; $P < 0.0001$) by control cells (Fig. 4*A* and *B*). H_2O_2 stimulated production of GS-HNE and GS-DHN was 4.7-fold ($P < 0.0001$) and 1.7-fold ($P < 0.01$) higher in control cells relative to KD cells, respectively. Basally, control cells produced 1.4-fold higher levels of GS-HNE ($P < 0.05$) than GSTA4 KD cells; however, GS-DHN production did not differ between control and KD (Fig. 4*A* and *B*).

In GSTA4 OE cells, H_2O_2 treatment resulted in increased production of GS-HNE (9-fold, from 150 ± 3 to 1,300 ± 60 pg/mL; $P < 0.0001$) and GS-DHN (17-fold, from 300 ± 20 to 5,000 ± 500 pg/mL; $P < 0.001$)

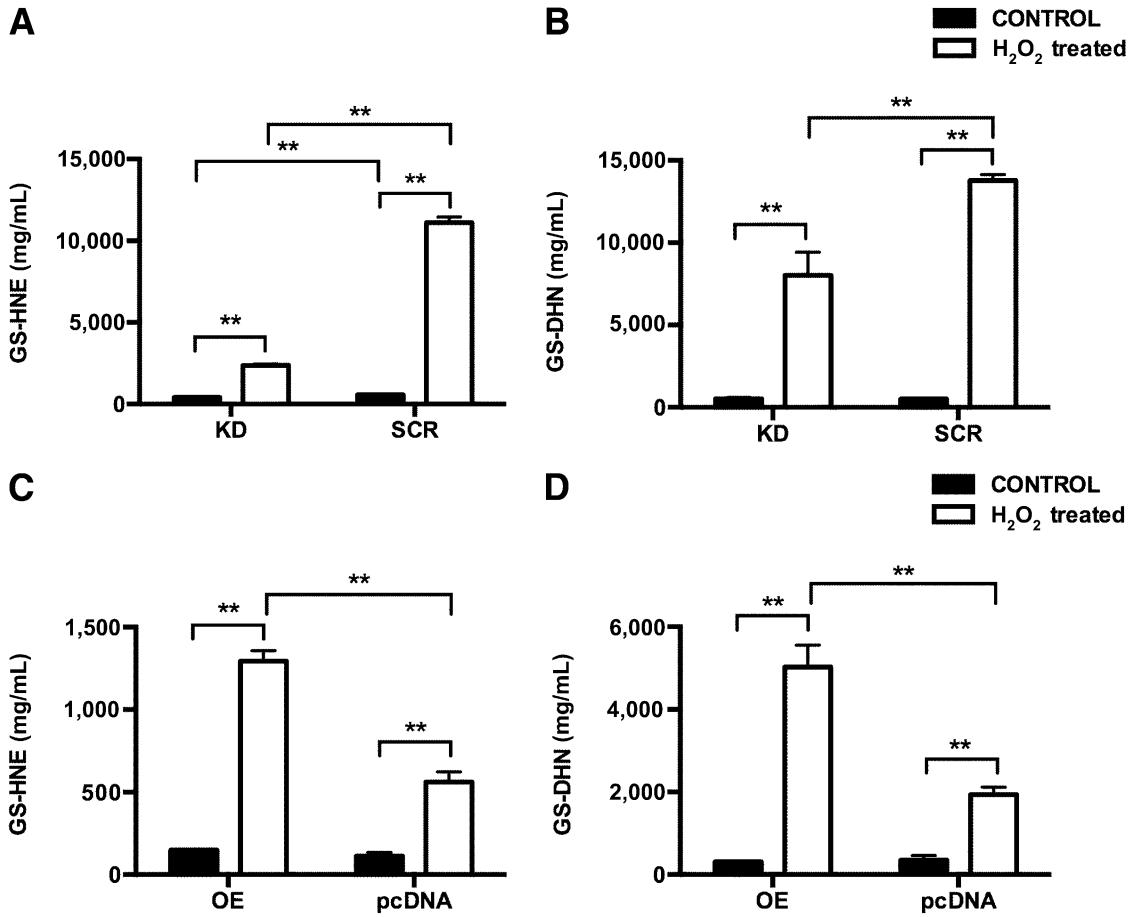

Figure 4—Effect of GSTA4 silencing or overproduction on generation of GS-HNE and GS-DHN by 3T3-L1 adipocytes. 3T3-L1 adipocytes were treated with control media or media containing 500 μmol/L H_2O_2 for 2 h, and medium was assayed for GS-HNE and GS-DHN using LC-MS/MS. *A*: GS-HNE production in 3T3-L1 control (scrambled [SCR]) or GSTA4 KD (KD) cells. *B*: GS-DHN production in 3T3-L1 control (SCR) or GSTA4 KD (KD) cells. *C*: GS-HNE production in 3T3-L1 control (pcDNA) or GSTA4 OE (OE) cells. *D*: GS-DHN production in 3T3-L1 control (pcDNA) or GSTA4 OE (OE) cells. $^*P < 0.05$, $^{**}P < 0.01$.

(Fig. 4*C* and *D*). Correlating with increased expression of GSTA4, this increase was significantly higher than the increase in GS-HNE (fivefold, from 110 ± 20 to 560 ± 60 pg/mL; $P < 0.001$) and GS-DHN (sixfold, from 350 ± 110 to 1,900 ± 180 pg/mL; $P < 0.001$) made by control cells. Compared with GSTA4 KD cells, GSTA4 OE cells had 2.3-fold ($P < 0.001$) and 2.6-fold ($P < 0.01$) higher production of GS-HNE and GS-DHN, respectively, in response to H_2O_2 relative to control cells (Fig. 4*C* and *D*). There was no significant difference between GSTA4 OE and control cells in basal formation of GS-HNE or GS-DHN (Fig. 4*C* and *D*).

Effect of GS-HNE/GS-DHN on Macrophage Inflammation

Because glutathione metabolites are produced by adipocytes and are hypothesized to induce inflammatory signaling cascades in macrophages, RAW 264.7 or primary peritoneal macrophages were pretreated with 1 μg/mL LPS and then incubated for 24 h with GS-HNE or GS-DHN to evaluate TNF-α secretion. Treatment of RAW 264.7 macrophages resulted in a dose-dependent increase in TNF-α secretion (Fig. 5*A*). Interestingly, treatment of primary peritoneal macrophages with GS-DHN, but not GS-HNE, resulted in increased TNF-α secretion (Fig. 5*B*). In contrast, neither GS-HNE nor GS-DHN treatment resulted in increased monocyte chemoattractant protein-1 or interleukin (IL)-6 production in macrophages (data not shown).

To further characterize the proinflammatory properties of glutathione metabolites, peritoneal macrophages were incubated with GS-HNE or GS-DHN for 2 h, and LTC_4 production was measured by LC-MS/MS. LTC_4 has been implicated as playing an inflammatory role in macrophage biology (26), and levels of LTC_4 increase in visceral adipose tissue with obesity (27). GS-HNE and GS-DHN both induced an approximately threefold increase in production of LTC_4 (Fig. 5*C*).

Given results showing GS-HNE and GS-DHN have proinflammatory signaling properties, a panel of proinflammatory genes was surveyed to provide a more complete evaluation of the role of glutathione

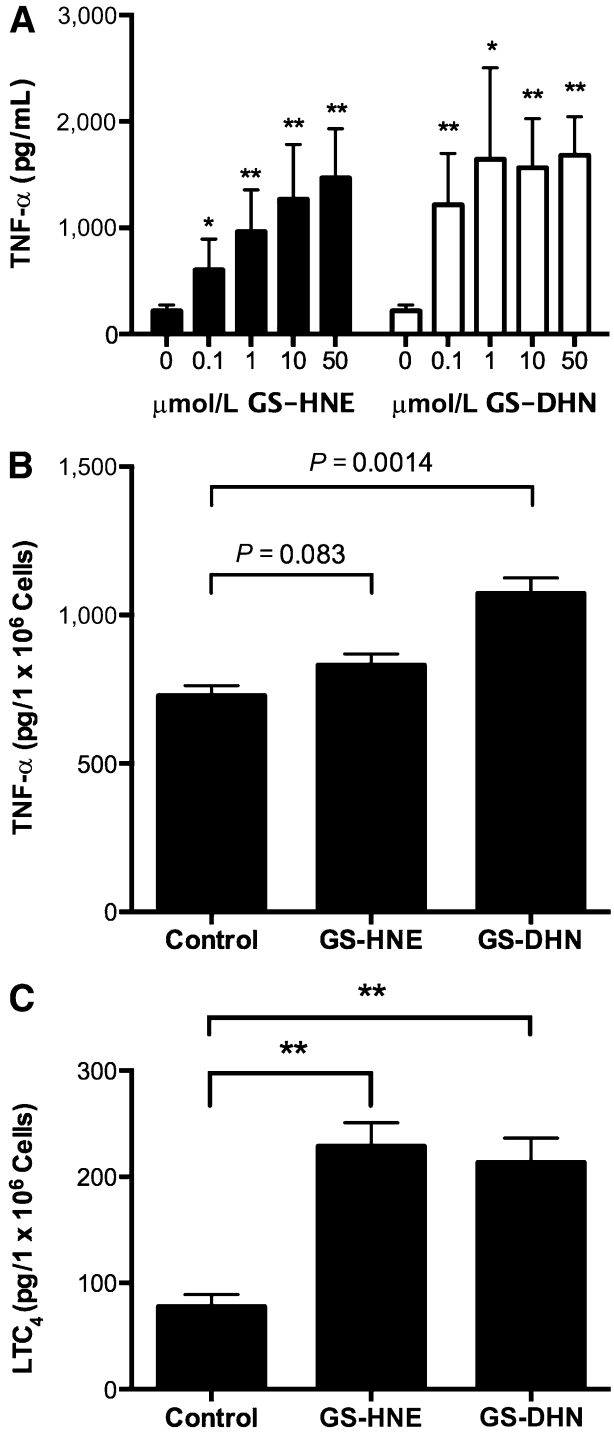

Figure 5—Effect of GS-HNE or GS-DHN treatment on production of inflammatory mediators. *A*: RAW 264.7 macrophages were treated with 1 μg/mL LPS for 18 h, followed by addition of increasing concentrations of GS-HNE or GS-DHN for 24 h, and TNF-α was assayed in the culture medium. *B*: Mouse peritoneal macrophages were pretreated with LPS, followed by treatment with 10 μmol/L GS-HNE or GS-DHN for 24 h, and TNF-α was assayed in the supernatant. *C*: Mouse peritoneal macrophages were pretreated with LPS, followed by treatment with 10 μmol/L GS-HNE or GS-DHN for 2 h, and LTC_4 was quantified in the media using LC-MS/MS. *$P < 0.05$, **$P < 0.01$.

metabolites in inflammation. Treatment of primary peritoneal macrophages with 10 μmol/L GS-HNE or GS-DHN after LPS stimulation resulted in significantly increased expression of C3, C4b, c-Fos, igtb2, Nfkb1, and Nos2. In addition, GS-HNE induced increased expression of Csf1 (macrophage colony–stimulating factor [MCSF]), IL23 receptor, Toll-like receptor (TLR) 6, and TLR9, whereas GS-DHN induced increased expression of CD40 (Fig. 6).

GS-HNE/GS-DHN in GSTA4 OE Mice

To examine the effect of fat-specific GSTA4 overexpression on whole body metabolism, transgenic mice were generated expressing HA-tagged GSTA4 under FABP4 promoter and express the transgene in white and brown adipose tissue (Supplementary Fig. 1). As has been previously described, expression of GSTA4 in visceral adipose tissue was significantly downregulated (70% reduction; $P < 0.05$) on a high-fat diet (14). In contrast, adipose GSTA4 mRNA level in transgenic mice was not decreased by high-fat feeding (Fig. 7*A*). Owing to the differential effect of the high-fat diet on GSTA4 expression, transgenic mice had 15-fold and 42-fold higher levels of GSTA4 mRNA expression in low-fat and high-fat diet, respectively (Fig. 7*A*). In parallel to this, transgenic mice had a fivefold higher rate of GSTA4 enzymatic activity (Fig. 7*B*) and an ~50% decrease in protein carbonylation in fat tissue (Fig. 7*C*). There was a trend toward higher levels of GS-HNE ($P = 0.17$) in epididymal adipose tissue of low fat–fed transgenic mice relative to wild-type mice but no difference in adipose GS-HNE content in high fat–fed transgenic mice relative to high fat–fed wild-type mice (data not shown). GS-DHN in epididymal adipose tissue was not different between transgenic and wild-type mice fed the low- or high-fat diet (data not shown).

GSTA4 transgenic mice fed a high-fat diet exhibited a significantly higher fasting blood glucose level (242 vs. 218 mg/dL, $P < 0.05$) but did not show a significant difference in weight compared with wild-type mice (data not shown). Glucose tolerance tests and insulin tolerance tests were performed on transgenic and wild-type mice fed a high-fat diet, and transgenic animals were mildly glucose-intolerant and had higher blood glucose on average at all time points (Fig. 8*A* and *B*). There was no difference in insulin tolerance tests between mouse strains.

DISCUSSION

Metabolism of α,β-unsaturated aldehydes by GST enzymes constitutes an important protective mechanism against oxidative damage to proteins, DNA, and lipids. Recent reports have characterized mitogenic and proinflammatory properties of GS-HNE and GS-DHN and their cell-permeable esters (19,20,28–30). Although these metabolites are products of the same pathway, GS-HNE, but not GS-DHN, induced peritoneal leukocyte

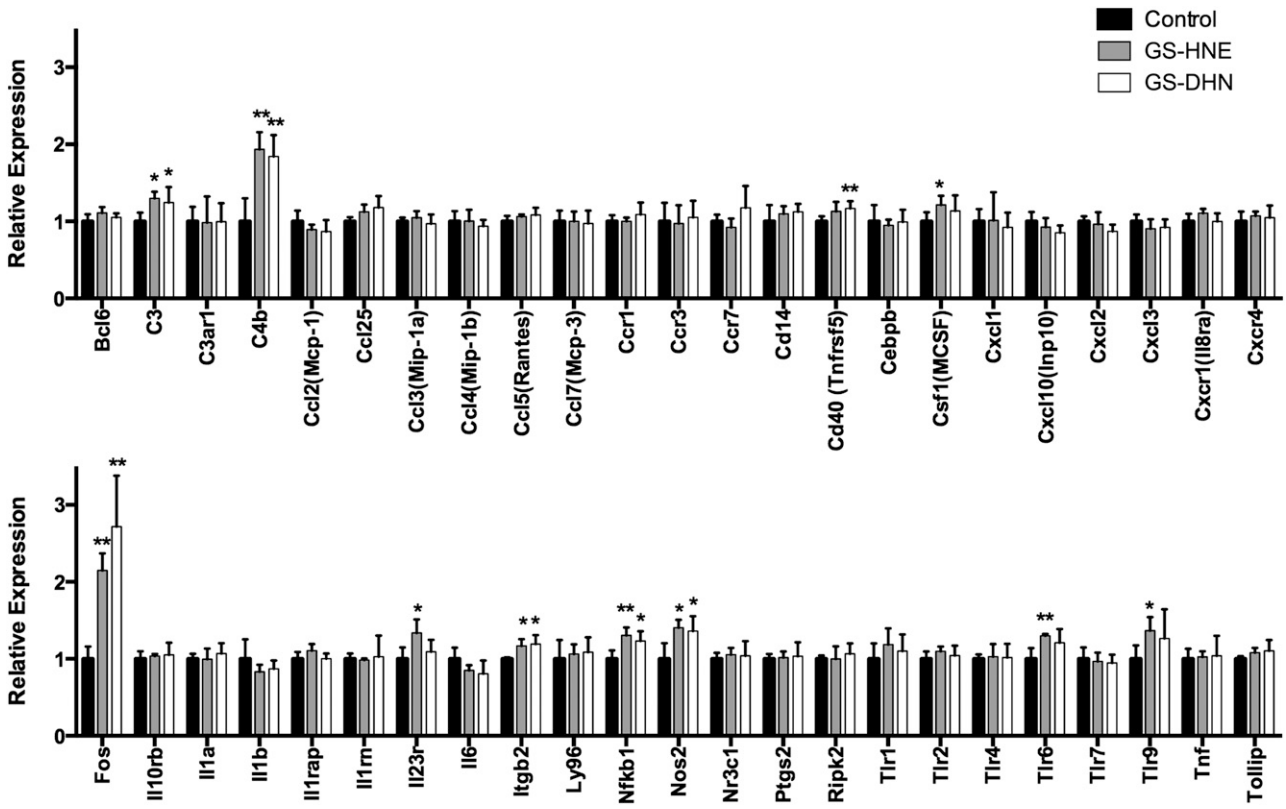

Figure 6—Expression of inflammatory genes in macrophages after treatment with GS-HNE or GS-DHN. Mouse peritoneal macrophages were treated with 1 μg/mL LPS for 18 h, followed by addition with control media, 10 μmol/L GS-HNE, or 10 μmol/L GS-DHN. After 24 h, the expression of cytokines and chemokines was analyzed using quantitative RT-PCR and normalized to control expression levels for each gene. *$P < 0.05$, **$P < 0.01$.

infiltration and proinflammatory lipid and cytokine production (19,30). In contrast, GS-DHN formed via aldose reductase has been shown to induce inflammation (18,31) and mediate cytotoxic activity (28) in macrophages and induce mitogenic signaling in smooth muscle (30). A role for GS-HNE and GS-DHN in adipose biology is suggested by observations in RLIP76 knockout mice in which export of glutathione metabolites is blocked. These mice are protected against inflammation and, notably, from oxidative stress–induced insulin resistance (32,33).

To evaluate the role of GS-HNE and GS-DHN in obesity-induced metabolic syndrome, GS-HNE and GS-DHN were measured in visceral adipose tissue. GS-HNE levels were significantly increased in high fat–fed and *ob/ob* mice compared with chow-fed mice. GS-DHN was increased in *ob/ob* mice but lacked statistical significance for high fat–fed mice despite a very large effect size due to individual variability in GS-DHN. Expression of aldose reductase, which reduces GS-HNE to form GS-DHN, is upregulated by the antioxidant regulator KEAP (34). Thus, a possible explanation for variation in GS-DHN levels may be variable antioxidant response and, thus, variable expression of this enzyme. Interestingly, these increases occurred despite the observation that GSTA4, the primary enzyme responsible for glutathionylation of 4-HNE, is downregulated ~90% during chronic overnutrition (14). This may represent a dramatic increase in lipid peroxidation with greater nonenzymatic formation of GS-HNE and GS-DHN and suggests these metabolites have the potential to maintain obesity-induced inflammation despite downregulation of GSTA4.

In vitro experimentation with macrophage and cultured adipocytes showed GS-HNE and GS-DHN production was increased in adipocytes, but not macrophages, in response to oxidative stress, suggesting adipocytes are responsible for oxidative stress–induced production of GS-HNE and GS-DHN in adipose tissue. To elucidate the oxidative stress response to overnutrition, 3T3-L1 adipocytes were grown in low- or high-glucose conditions. High glucose induced greater lipid accumulation in adipocytes, mirroring lipid accumulation in adipose tissue during chronic overnutrition. Growing 3T3-L1 adipocytes in high-glucose conditions alone did not result in increased GS-HNE or GS-DHN production. However, H_2O_2 with high glucose synergistically increased GS-HNE and GS-DHN, suggesting high glucose exposure potentiates cells toward increased oxidative stress and lipid peroxidation. The mechanism for this potentiation is not clear and may be due to increased reactive oxygen species production, increased lipid

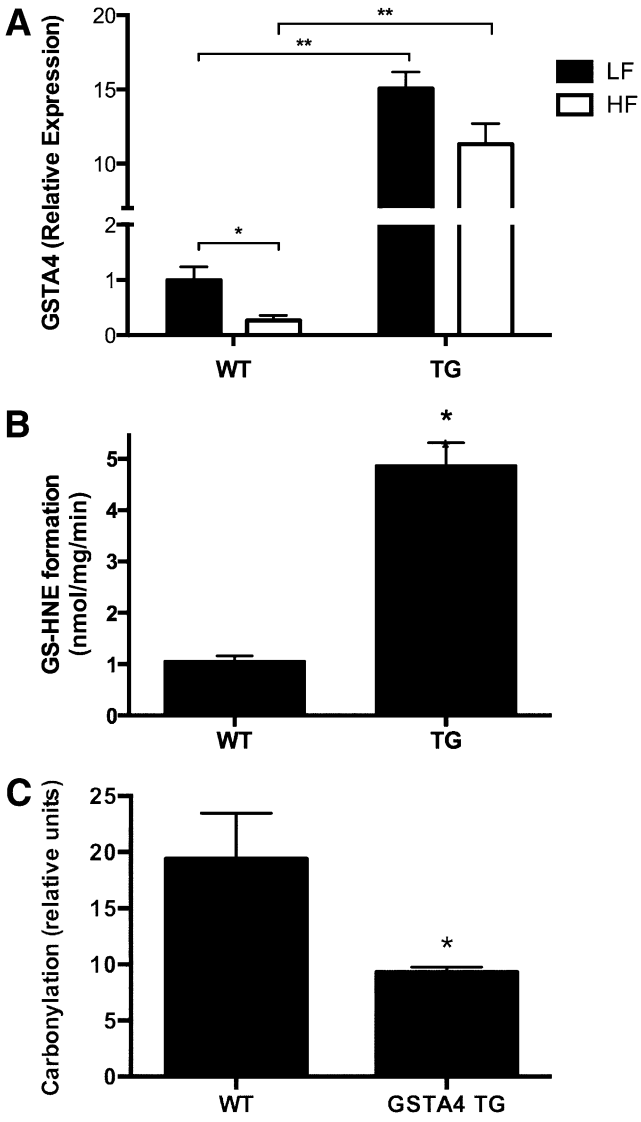

Figure 7—GSTA4 expression and activity in transgenic (TG) mouse adipose tissue. *A*: Relative gene expression of GSTA4 in adipose tissue from wild-type (WT) mice or GSTA4 TG (HA-GSTA4) mice fed a low-fat (LF) and high-fat (HF) diet. *B*: GSTA4 enzyme activity in tissues of WT mice or GSTA4 TG (HA-GSTA4) mice by LC-MS/MS. *C*: Protein carbonylation in visceral adipose tissue of WT and HA-GSTA4 TG mice. Protein from WT C57Bl/6J and HA-GSTA4 TG mice (n = 6–7) was analyzed for carbonylation adducts using biotin-hydrazide, as described (14). $^{*}P < 0.05$, $^{**}P < 0.01$. WT, wild-type.

substrate for lipid peroxidation, or both. Experiments with GSTA4-silenced and OE 3T3-L1 adipocytes demonstrated oxidative-stress induced production of GS-HNE and GS-DHN was dependent on GSTA4 expression, supporting the conclusion that GSTA4 is the primary enzyme responsible for the regulation of production of GS-HNE and GS-DHN.

Although both glutathionyl lipid aldehydes induced dose-dependent increases in TNF-α production by macrophages in culture, GS-DHN was effective at lower concentrations than GS-HNE. Primary peritoneal macrophages produced TNF-α in response to GS-DHN, but response to GS-HNE was weaker and not statistically significant. The more potent induction of the inflammatory cytokine TNF-α by GS-DHN is consistent with previous studies showing GS-DHN, but not GS-HNE, is responsible for inducing macrophage production of inflammatory mediators (31). In contrast, production of LTC_4 by peritoneal macrophages was similar in response to GS-HNE or GS-DHN. Differential activity of GS-HNE and GS-DHN may indicate differences in their role in acute inflammatory response, as characterized by LTC_4 production (35) versus chronic inflammation as characterized by TNF-α (36). Induction of macrophage production of TNF-α (37,38) by GS-DHN represents a potential direct mechanism by which adipocyte oxidative stress may induce macrophage inflammation via intercellular cross talk. The role and relative importance of GS-HNE are less clear, but one possibility is an indirect chemotactic mechanism as LTC_4 induces vascular permeability, contributing to immune cell infiltration (39), consistent with previously identified chemotactic activity of GS-HNE in the peritoneum (19).

Increased TNF-α and LTC_4 production provide evidence that glutathionyl lipid aldehydes display chronic and acute proinflammatory properties. To broaden characterization of these inflammatory properties, RNA from primary peritoneal macrophages treated with GS-DHN or GS-HNE was assessed by proinflammatory microarray analysis. GS-HNE and GS-DHN both increase C3, C4b, Nos2 (inducible nitric oxide synthase), NF-κB1, Igtb2, and c-FOS. C3 and C4b are important in the complement cascade and contribute to the innate immune response (40). Nos2 and NF-κB1 are involved in increasing proinflammatory gene expression (41,42). Igtb2 is found in myeloid cells and is associated with the innate immune response of macrophages (43). Fos interacts with TLR signaling pathways, contributing to inflammatory response (44). In addition, GS-HNE, but not GS-DHN, induced increased expression of MCSF, IL23R, TLR6, and TLR9. MCSF is involved in differentiation of peripheral monocytes into macrophages and is important in M1 polarization of macrophages, a proinflammatory phenotype (45). IL23R is associated with a number of autoimmune disorders (46). TLR6 and TLR9 are involved in pathogen recognition and innate immune response (47). GS-DHN, but not GS-HNE, induced increased expression of CD40, which is found on antigen-presenting cells and is a member of the TNF receptor superfamily that binds interferon-γ (48). Taken together, these array data indicate that GS-HNE and GS-DHN induce an inflammatory response via expression of a number of genes involved in the innate immune response and infiltration and polarization of macrophages to a proinflammatory phenotype.

To study the role of GSTA4 in the development of insulin resistance, transgenic mice OE GSTA4 were fed a high-fat diet. Although transgenic mice became

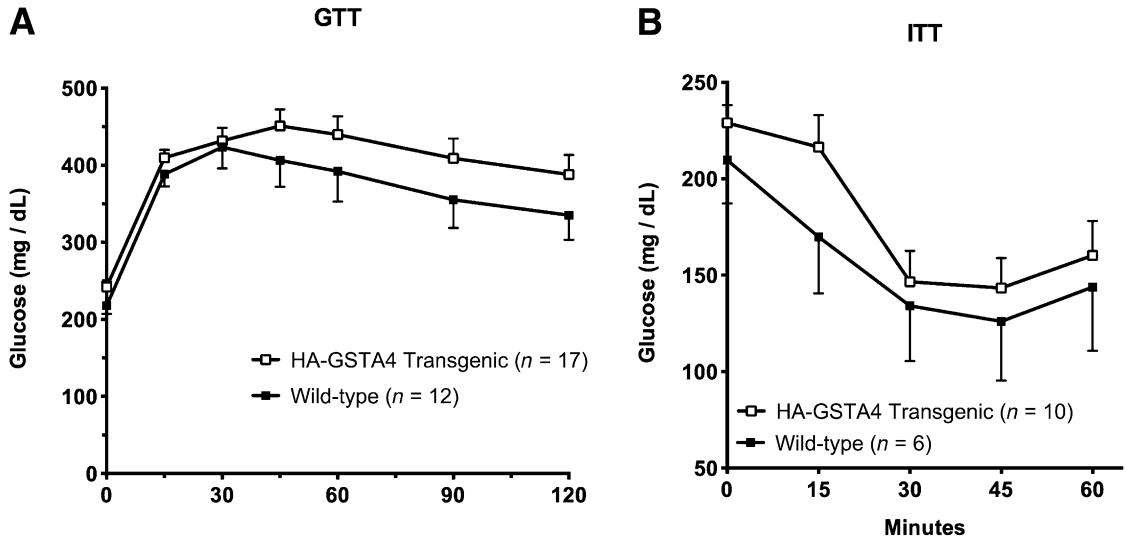

Figure 8—Effect of GSTA4 overexpression in mouse adipose tissue on glucose and insulin tolerance. Wild-type and GSTA4 OE transgenic mice (HA-GSTA4) maintained on a high-fat diet for 12 weeks were evaluated by glucose tolerance test (GTT; n = 12–17) (*A*) and insulin tolerance test (ITT; n = 6–10) (*B*).

similarly obese and activity of GSTA4 was higher in transgenic fat, actual levels of GS-HNE and GS-DHN were not significantly higher in their adipose tissue, relative to wild-type mice. Because glutathionyl lipid aldehydes are actively transported out of the cell into the bloodstream, further metabolized in the kidney, and excreted, the content of tissue at any given time likely largely represents steady-state levels in the extracellular matrix and local tissue vasculature, with a relatively small intracellular content. This may explain the discrepancy between increased GSTA4 capacity and unchanged levels of its product in transgenic mice relative to wild-type mice. Another possibility is limitation of GS-HNE and GS-DHN production by the precursor 4-HNE, which may be equally elevated in wild-type and transgenic mice. In contrast, the differences seen in GS-HNE content in mice fed a high-fat diet relative to mice fed chow is consistent with both increased 4-HNE production and increased fat tissue mass.

Despite unchanged tissue GS-HNE and GS-DHN content, fasting blood glucose was significantly higher in transgenic mice. This difference may indicate that although adipose GS-HNE and GS-DHN levels are unchanged, increased GSTA4 activity results in increased efflux of glutathionyl lipid aldehydes from adipocytes and increased exposure of tissue-resident macrophages to these inflammatory mediators. Action of GS-HNE on chemotaxis of inflammatory cells or GS-DHN on activation of macrophages may contribute to the development of insulin resistance.

Interestingly, GSTA4-null mice, although showing an increased steady-state level of 4-HNE in their tissues (49), were noted to have an extended life span (50) that was attributed to an associated increase in antioxidant response (50). Studies described here suggest decreased inflammation may be an alternate explanation, supported by the observation that GSTA4-null mice show greater susceptibility to bacterial infection (49), an indication of reduced immune function.

These results suggest a novel mechanism for development of obesity-induced metabolic syndrome in which oxidative stress in adipocytes results in increased production of GS-HNE and GS-DHN, inducing a macrophage inflammatory response. Induction of inflammatory cytokines and lipids then feeds forward to adipocytes, inducing insulin resistance and metabolic dysfunction. This model provides a plausible mechanism for oxidative stress-induced inflammation via intercellular cross talk. Furthermore, obesity-induced decreases in GSTA4 expression may be a compensatory response, supporting the concept that downregulation of GSTA4 is an adaptive mechanism designed to decrease the inflammatory cascade induced by GS-HNE and GS-DHN.

Acknowledgments. The authors thank the members of the Bernlohr laboratory for helpful suggestions during the preparation of this manuscript and the members of the University of Minnesota Center for Mass Spectrometry and Proteomics (Minneapolis, MN) for their assistance with lipid analysis.

Funding. Research reported in this study was supported by the National Institutes of Health (NIH) under grants DK-084669 and DK-053189 to D.A.B., P30-DK-050456 to B.I.F., and F32-DK-091004 to E.K.L. The content is solely the responsibility of the authors and does not necessarily represent the official views of the NIH.

Duality of Interest. No potential conflicts of interest relevant to this article were reported.

Author Contributions. B.I.F. and E.K.L. researched data, performed analysis and interpretation, and wrote the manuscript. W.S.H. developed the

mouse model, researched data, performed analysis and interpretation, contributed to discussion, and reviewed and edited the manuscript. D.A.B. developed the overall research plan, contributed to analysis and interpretation, and reviewed and edited the manuscript. D.A.B. is the guarantor of this work, and, as such, had full access to all the data in the study and takes responsibility for the integrity of the data and the accuracy of the data analysis.

Prior Presentation. Parts of this study were presented in abstract form at the Joint Meeting of Pediatric Endocrinology, Milan, Italy, 20 September 2013.

References

1. Gutierrez DA, Puglisi MJ, Hasty AH. Impact of increased adipose tissue mass on inflammation, insulin resistance, and dyslipidemia. Curr Diab Rep 2009;9:26–32
2. Curtis JM, Grimsrud PA, Wright WS, et al. Downregulation of adipose glutathione S-transferase A4 leads to increased protein carbonylation, oxidative stress, and mitochondrial dysfunction. Diabetes 2010;59:1132–1142
3. Furukawa S, Fujita T, Shimabukuro M, et al. Increased oxidative stress in obesity and its impact on metabolic syndrome. J Clin Invest 2004;114:1752–1761
4. Houstis N, Rosen ED, Lander ES. Reactive oxygen species have a causal role in multiple forms of insulin resistance. Nature 2006;440:944–948
5. Andriantsitohaina R, Duluc L, García-Rodríguez JC, et al. Systems biology of antioxidants. Clin Sci (Lond) 2012;123:173–192
6. Boden MJ, Brandon AE, Tid-Ang JD, et al. Overexpression of manganese superoxide dismutase ameliorates high-fat diet-induced insulin resistance in rat skeletal muscle. Am J Physiol Endocrinol Metab 2012;303:E798–E805
7. Huh JY, Kim Y, Jeong J, et al. Peroxiredoxin 3 is a key molecule regulating adipocyte oxidative stress, mitochondrial biogenesis, and adipokine expression. Antioxid Redox Signal 2012;16:229–243
8. Shi Q, Gibson GE. Oxidative stress and transcriptional regulation in Alzheimer disease. Alzheimer Dis Assoc Disord 2007;21:276–291
9. Mandelker L. Introduction to oxidative stress and mitochondrial dysfunction. Vet Clin North Am Small Anim Pract 2008;38:1–30, v
10. Uchida K. 4-Hydroxy-2-nonenal: a product and mediator of oxidative stress. Prog Lipid Res 2003;42:318–343
11. Carini M, Aldini G, Facino RM. Mass spectrometry for detection of 4-hydroxy-trans-2-nonenal (HNE) adducts with peptides and proteins. Mass Spectrom Rev 2004;23:281–305
12. Curtis JM, Hahn WS, Stone MD, et al. Protein carbonylation and adipocyte mitochondrial function. J Biol Chem 2012;287:32967–32980
13. Demozay D, Mas J-C, Rocchi S, Van Obberghen E. FALDH reverses the deleterious action of oxidative stress induced by lipid peroxidation product 4-hydroxynonenal on insulin signaling in 3T3-L1 adipocytes. Diabetes 2008;57:1216–1226
14. Grimsrud PA, Picklo MJ Sr, Griffin TJ, Bernlohr DA. Carbonylation of adipose proteins in obesity and insulin resistance: identification of adipocyte fatty acid-binding protein as a cellular target of 4-hydroxynonenal. Mol Cell Proteomics 2007;6:624–637
15. Poli G, Biasi F, Leonarduzzi G. 4-Hydroxynonenal-protein adducts: A reliable biomarker of lipid oxidation in liver diseases. Mol Aspects Med 2008;29:67–71
16. Singhal SS, Yadav S, Roth C, Singhal J. RLIP76: A novel glutathione-conjugate and multi-drug transporter. Biochem Pharmacol 2009;77:761–769
17. Awasthi S, Cheng J, Singhal SS, et al. Novel function of human RLIP76: ATP-dependent transport of glutathione conjugates and doxorubicin. Biochemistry 2000;39:9327–9334
18. Ramana KV, Srivastava SK. Mediation of aldose reductase in lipopolysaccharide-induced inflammatory signals in mouse peritoneal macrophages. Cytokine 2006;36:115–122
19. Spite M, Summers L, Porter TF, Srivastava S, Bhatnagar A, Serhan CN. Resolvin D1 controls inflammation initiated by glutathione-lipid conjugates formed during oxidative stress. Br J Pharmacol 2009;158:1062–1073
20. Ramana KV, Bhatnagar A, Srivastava S, et al. Mitogenic responses of vascular smooth muscle cells to lipid peroxidation-derived aldehyde 4-hydroxy-trans-2-nonenal (HNE): role of aldose reductase-catalyzed reduction of the HNE-glutathione conjugates in regulating cell growth. J Biol Chem 2006;281:17652–17660
21. Matarese V, Bernlohr DA. Purification of murine adipocyte lipid-binding protein. Characterization as a fatty acid- and retinoic acid-binding protein. J Biol Chem 1988;263:14544–14551
22. Student AK, Hsu RY, Lane MD. Induction of fatty acid synthetase synthesis in differentiating 3T3-L1 preadipocytes. J Biol Chem 1980;255:4745–4750
23. Long EK, Rosenberger TA, Picklo MJ Sr. Ethanol withdrawal increases glutathione adducts of 4-hydroxy-2-hexenal but not 4-hydroxyl-2-nonenal in the rat cerebral cortex. Free Radic Biol Med 2010;48:384–390
24. Padmalayam I. Targeting mitochondrial oxidative stress through lipoic acid synthase: a novel strategy to manage diabetic cardiovascular disease. Cardiovasc Hematol Agents Med Chem 2012;10:223–233
25. Lin Y, Berg AH, Iyengar P, et al. The hyperglycemia-induced inflammatory response in adipocytes: the role of reactive oxygen species. J Biol Chem 2005;280:4617–4626
26. Wenzel SE, Trudeau JB, Riches DW, Westcott JY, Henson PM. Peritoneal lavage fluid alters patterns of eicosanoid production in murine bone marrow-derived and peritoneal macrophages: dependency on inflammatory state of the peritoneum. Inflammation 1993;17:743–756
27. Long EK, Hellberg K, Foncea R, Hertzel AV, Suttles J, Bernlohr DA. Fatty acids induce leukotriene C4 synthesis in macrophages in a fatty acid binding protein-dependent manner. Biochim Biophys Acta 2013;1831:1199–1207
28. Ramana KV, Reddy ABM, Tammali R, Srivastava SK. Aldose reductase mediates endotoxin-induced production of nitric oxide and cytotoxicity in murine macrophages. Free Radic Biol Med 2007;42:1290–1302
29. Tammali R, Ramana KV, Srivastava SK. Aldose reductase regulates TNF-alpha-induced PGE2 production in human colon cancer cells. Cancer Lett 2007;252:299–306
30. Srivastava S, Ramana KV, Bhatnagar A, Srivastava SK. Synthesis, quantification, characterization, and signaling properties of glutathionyl conjugates of enals. Methods Enzymol 2010;474:297–313
31. Ramana KV, Fadl AA, Tammali R, Reddy ABM, Chopra AK, Srivastava SK. Aldose reductase mediates the lipopolysaccharide-induced release of inflammatory mediators in RAW264.7 murine macrophages. J Biol Chem 2006;281:33019–33029
32. Engle MR, Singh SP, Czernik PJ, et al. Physiological role of mGSTA4-4, a glutathione S-transferase metabolizing 4-hydroxynonenal: generation and analysis of mGsta4 null mouse. Toxicol Appl Pharmacol 2004;194:296–308
33. Singh SP, Niemczyk M, Saini D, Sadovov V, Zimniak L, Zimniak P. Disruption of the mGsta4 gene increases life span of C57BL mice. J Gerontol A Biol Sci Med Sci 2010;65:14–23
34. Jung K-A, Choi B-H, Nam C-W, et al. Identification of aldo-keto reductases as NRF2-target marker genes in human cells. Toxicol Lett 2013;218:39–49

35. Eun JC, Moore EE, Mauchley DC, et al. The 5-lipoxygenase pathway is required for acute lung injury following hemorrhagic shock. Shock 2012; 37:599–604

36. Popa C, Netea MG, van Riel PLCM, van der Meer JWM, Stalenhoef AFH. The role of TNF-alpha in chronic inflammatory conditions, intermediary metabolism, and cardiovascular risk. J Lipid Res 2007;48:751–762

37. Parameswaran N, Patial S. Tumor necrosis factor-α signaling in macrophages. Crit Rev Eukaryot Gene Expr 2010;20:87–103

38. Serrano-Marco L, Chacón MR, Maymó-Masip E, et al. TNF-α inhibits PPARβ/δ activity and SIRT1 expression through NF-κB in human adipocytes. Biochim Biophys Acta 2012;1821:1177–1185

39. Hui Y, Cheng Y, Smalera I, et al. Directed vascular expression of human cysteinyl leukotriene 2 receptor modulates endothelial permeability and systemic blood pressure. Circulation 2004;110:3360–3366

40. Ballanti E, Perricone C, Greco E, et al. Complement and autoimmunity. Immunol Res 2013;56:477–491

41. Korhonen R, Lahti A, Kankaanranta H, Moilanen E. Nitric oxide production and signaling in inflammation. Curr Drug Targets Inflamm Allergy 2005;4: 471–479

42. Müller-Ladner U, Gay RE, Gay S. Role of nuclear factor kappaB in synovial inflammation. Curr Rheumatol Rep 2002;4:201–207

43. Jennings MP, Srikhanta YN, Moxon ER, et al. The genetic basis of the phase variation repertoire of lipopolysaccharide immunotypes in *Neisseria meningitidis*. Microbiology 1999;145:3013–3021.

44. Wagner EF, Eferl R. Fos/AP-1 proteins in bone and the immune system. Immunol Rev 2005;208:126–140

45. Lagrange B, Martin RZ, Droin N, et al. A role for miR-142-3p in colony-stimulating factor 1-induced monocyte differentiation into macrophages. Biochim Biophys Acta 2013;1833:1936–1946

46. Vandenbroeck K. Cytokine gene polymorphisms and human autoimmune disease in the era of genome-wide association studies. J Interferon Cytokine Res 2012;32:139–151

47. Hallman M, Rämet M, Ezekowitz RA. Toll-like receptors as sensors of pathogens. Pediatr Res 2001;50:315–321

48. Benveniste EN, Nguyen VT, Wesemann DR. Molecular regulation of CD40 gene expression in macrophages and microglia. Brain Behav Immun 2004; 18:7–12

49. Awasthi S, Singhal SS, Yadav S, et al. A central role of RLIP76 in regulation of glycemic control. Diabetes 2010;59:714–725

50. Singhal J, Nagaprashantha L, Vatsyayan R, Awasthi S, Singhal SS. RLIP76, a glutathione-conjugate transporter, plays a major role in the pathogenesis of metabolic syndrome. PLoS ONE 2011;6:e24688